

The Energy of a Moving Quark-Antiquark Pair in an $\mathcal{N} = 4$ SYM Plasma

Mariano Chernicoff*, J. Antonio García† and Alberto Güijosa‡

Departamento de Física de Altas Energías, Instituto de Ciencias Nucleares

Universidad Nacional Autónoma de México

Apdo. Postal 70-543, México D.F. 04510

Abstract

We make use of the AdS/CFT correspondence to determine the energy of an external quark-antiquark pair that moves through strongly-coupled thermal $\mathcal{N} = 4$ super-Yang-Mills plasma, both in the rest frame of the plasma and in the rest frame of the pair. It is found that the pair feels no drag force, has an energy that reproduces the expected $1/L$ (or γ/L) behavior at small quark-antiquark separations, and becomes unbound beyond a certain screening length whose velocity-dependence we determine. We discuss the relation between the high-velocity limit of our results and the lightlike Wilson loop proposed recently as a definition of the jet-quenching parameter.

1 Introduction and Summary

In the past few months, the use of the AdS/CFT correspondence [1, 2, 3] to study energy loss in finite-temperature strongly-coupled gauge theories has attracted significant attention, partly because it is hoped that this line of research could eventually make contact with experimental data from RHIC [4] and ALICE [5].

The drag force experienced by a heavy quark that moves through a thermal $\mathcal{N} = 4$ super-Yang-Mills (SYM) plasma was determined in [6, 7], using its dual description as a string that moves on an AdS-Schwarzschild background. The same information was obtained independently in [8] through a different method, based on an analysis of small string fluctuations (a similar calculation was performed in [6]). Generalizations of the first calculation may be found in [9, 10, 11]. A comparison with the corresponding weakly-coupled result was carried out in [12]. The connection with magnetic confinement was explored in [13]. The directionality of the coherent wake

*e-mail: mariano@nucleares.unam.mx

†e-mail: garcia@nucleares.unam.mx

‡e-mail: alberto@nucleares.unam.mx

left by the moving quark on the gluonic fields was studied in [14, 15, 16], using the methods of [17, 18].

An independent approach has aimed at determining the jet-quenching parameter \hat{q} that in phenomenological models of energy loss through medium-induced radiation is meant to codify the average squared transverse momentum transferred to the quark by the medium (for reviews see [19, 20]). Based on the fact that certain approximate calculations in these models relate \hat{q} to a lightlike Wilson loop in the adjoint representation (see [20] and references therein), the authors of [21] suggested that this Wilson loop could be taken to provide a non-perturbative definition of the jet-quenching parameter. Using the simple large- N relation between adjoint and fundamental loops, and the AdS/CFT recipe for the latter¹ [23], they then proceeded to compute this parameter for $\mathcal{N} = 4$ SYM. Their calculation has been generalized in various directions in [24, 25, 11, 28, 29, 30]. Previous related work may be found in [26, 27].

Just like the drag force determination in [6, 7], the calculation of \hat{q} in [21] focuses on a string that moves on an AdS-Schwarzschild background. The difference is that the string considered in [6, 7] has a single endpoint on the boundary, representing the moving external quark, whereas the string studied in [21] has both of its endpoints on the boundary, representing an external quark-antiquark pair that traces out the required lightlike Wilson loop.

In this paper we perform a natural generalization of the above calculations, using the AdS/CFT correspondence to determine the energy of a quark-antiquark pair that moves with velocity v through a strongly-coupled thermal $\mathcal{N} = 4$ SYM plasma. This problem had been previously studied in the case $v = 0$, where the pair is static with respect to the plasma. As expected, the quark-antiquark potential was found to be insensitive to the plasma at small distances, and to display screening behavior beyond a certain length [31, 32]. Analyzing the manner in which these features are modified by the motion of the pair through the plasma is an interesting question in its own right, both from the theoretical and the phenomenological perspectives. Our analysis is additionally motivated by the current discussion on energy loss: the moving quark-antiquark pair serves as a color-neutral probe of the plasma that stands in useful contrast with the solitary quark considered in [6, 7], and moreover, in the $v \rightarrow 1$ limit it would be expected to make contact with the system studied in [21].

Our presentation is organized as follows. In Section 2 we briefly review the salient points of the drag force calculation of [6, 7], and then set up and study the analogous problem for the string on AdS-Schwarzschild that has both of its endpoints on the boundary, satisfying the boundary conditions (11). Below this equation and again after (19) we find that this string feels no drag force, discuss the physical reasons for this result and point out that there exist configurations with the same boundary conditions but different initial conditions where the string *does* experience a drag force. Although framed in the specific context of the background dual to $\mathcal{N} = 4$ SYM, the essence of our arguments is more general and applies to other backgrounds.

¹An AdS/CFT prescription for directly computing certain Wilson loops in an arbitrary representation of the gauge group was given recently in [22].

At the end of Section 2 we derive the basic equations (20)-(32) that determine the shape and energy of the string in the background at hand. We work first in the frame where the plasma is at rest, and discuss a subtlety in defining the energy (and momentum) of the disconnected strings dual to an unbound quark and antiquark. We then Lorentz-transform to the frame where the $q\bar{q}$ pair is at rest, where the energy can be defined in the standard straightforward manner. We note that even though the string is by definition static in this frame, it still carries momentum, which as we explain below (39) codifies information about the momentum density of the gluonic field configuration set up by the quarks in the dual gauge theory. Because of this non-vanishing momentum, the energy E in the plasma rest frame is not simply proportional to the energy \bar{E} in the pair rest frame. The relation between the two is given in (40).

Section 3 contains our main results, in SYM language. We open with a discussion on the gauge-theoretic interpretation for the result that the quark-antiquark pair feels no drag force as it ploughs through the $\mathcal{N} = 4$ SYM plasma. After that we carry out the numerical integrations needed to determine the energy of the $q\bar{q}$ pair as a function of the separation L and velocity v . The results are shown in Figs. 3,4. The energy reduces to the expected Coulombic behavior (46) for small separations, and then rises above this behavior due to the effects of the plasma, up to a screening length $L_*(v)$ beyond which the quark and antiquark become unbound. The velocity-dependence of this screening length is shown in Fig. 5; we find it to be well-approximated by (52). For velocities $v > 0.447$ we find a gap in energy between the bound and unbound $q\bar{q}$ configurations, whose physical significance remains unclear to us.

In the closing pages of Section 3 we discuss at length the relation between the $v \rightarrow 1$ limit of our results and the lightlike Wilson loop proposed in [21] as a definition of the jet-quenching parameter \hat{q} . The main lesson is that the AdS/CFT result of [21] cannot be obtained as a smooth limit of standard Wilson loops (11) with $v \rightarrow 1$ from below. We suggest that it should be regarded instead as arising from an approach to $v = 1$ from above. Finally, we note in (56) that, despite the fact that one cannot continuously interpolate between the spacelike worldsheet considered in [21] and the timelike worldsheets studied in the present paper, the $E \propto L^2$ dependence that is central to the definition of the parameter \hat{q} in [21] is in fact available in the $v \rightarrow 1$ limit of a subset of the configurations analyzed here. By analogy with [21], one can then define a parameter \mathcal{K} that, at least in this specific example, captures exactly the same information as (and is in close numerical agreement with) \hat{q} .

In the course of our investigation two related papers were posted on the arXiv. While our work was in progress, the paper [33] appeared, whose Section 4.2 discusses drag effects for mesons with spin in a certain confining non-supersymmetric gauge theory, arriving at conclusions which coincide with those of our Section 2. While the first version of our paper was in preparation, the work [34] appeared, which analyzes exactly the same quark-antiquark system as we do, focusing on the velocity-dependence of the screening length (for an arbitrary angle θ between the direction of motion and the quark-antiquark separation L), which we determine (for $\theta = \pi/2$)

in our Section 3. Their numerical results are in complete agreement with ours, but as discussed above (52), their definition of the screening length differs from ours for velocities $v < 0.447$. We should also note two additional developments that took place after the first version of this paper had appeared: first, the addition of a plot to [33] (Fig. 16), showing a meson size that scales with velocity in a manner compatible with the results for the screening length obtained in [34] and the present paper; second, the appearance of the work [42], which generalizes the screening length calculation to a large class of backgrounds, arriving at an analytic determination of the velocity-dependence in the ultra-relativistic regime.

2 Nambu-Goto String in AdS-Schwarzschild

As mentioned in the Introduction, the computation in [6, 7] of the drag force felt by an external quark moving through $\mathcal{N} = 4$ SYM plasma focuses on a string that extends all the way from the boundary to the horizon of an AdS-Schwarzschild geometry, i.e., from $r \rightarrow \infty$ to $r = r_H$, with r an appropriate radial coordinate that we will henceforth also use as spatial worldsheet coordinate. We will in addition employ the boundary time $t = x^0$ as worldsheet time, so altogether we work in the static gauge

$$\sigma = r, \quad \tau = t . \quad (1)$$

The dynamics of the string are described by the Nambu-Goto action

$$S = -\frac{1}{2\pi\alpha'} \int d\tau d\sigma \sqrt{-\det g_{\alpha\beta}} \equiv \frac{1}{2\pi\alpha'} \int d\tau d\sigma \mathcal{L} , \quad (2)$$

where $G_{\mu\nu}$ is the the spacetime metric and $g_{\alpha\beta} \equiv G_{\mu\nu} \partial_\alpha X^\mu \partial_\beta X^\nu$ the induced worldsheet metric. The force that a given segment of the string exerts along spatial direction i on the neighboring segment was expressed in [7] as

$$F_i = \frac{1}{2\pi\alpha'} \sqrt{-g} P_i^r , \quad (3)$$

with

$$P_\mu^\alpha = -g^{\alpha\beta} \partial_\beta X_\mu \quad (4)$$

the worldsheet current associated with spacetime momentum, whereas in [6] it was formulated as

$$F_i = \frac{1}{2\pi\alpha'} \Pi_i^r , \quad (5)$$

with

$$\Pi_\mu^\alpha = \frac{\partial \mathcal{L}}{\partial(\partial_\alpha X^\mu)} \quad (6)$$

the canonical momentum densities conjugate to X^μ . By explicitly inverting the 2×2 matrix $g_{\alpha\beta}$, one can easily verify that

$$\sqrt{-g} P_\mu^\alpha = \Pi_\mu^\alpha , \quad (7)$$

and so the expressions (3) and (5) coincide. Clearly the latter is simpler to use in explicit computations.

The crucial point in the calculation of [6, 7] is the observation that, if this string is assumed to travel at constant velocity $v \neq 0$ along a direction $x = x^1$ parallel to the boundary, then there is a certain velocity-dependent value of the radial coordinate,

$$r_v = \frac{r_H}{(1 - v^2)^{1/4}}, \quad (8)$$

below which the embedding function

$$X(r, t) = vt + \xi(r) \quad (9)$$

for the string would become imaginary. The only way to avoid this is to let the string trail behind its boundary endpoint following a specific profile $\xi(r) \neq \text{constant}$, which translates into a specific value for the drag force F_x exerted on the endpoint. In short, the non-zero value of the drag force is set uniquely by the condition that the string crosses the critical radius r_v .

In this section we are interested in exploring how these considerations generalize to a moving string that has *both* of its endpoints on the boundary, and is therefore dual not to a single quark but to a quark-antiquark pair in the gauge theory.

Since the string now extends first away from and then back to the boundary, the static gauge choice $\sigma = r$ leads of course to a double-valued parametrization, but this poses no problem other than the need to check by hand that the two halves of the string join together smoothly (which ensures that the action is extremized not just piecewise, but over the entire worldsheet). To describe a moving quark-antiquark pair, both of the string endpoints are taken to travel with the same velocity v in the x direction, and to be separated by a constant distance L along a certain boundary direction $y = x^2$. In other words, with a convenient choice of origin, the embedding functions (9) and

$$Y(r, t) = Y(r) \quad (10)$$

satisfy the boundary conditions

$$X(\infty, t) = vt, \quad Y(\infty) = \mp \frac{L}{2}, \quad (11)$$

where the upper (lower) signs refer to the left (right) half of the string. For concreteness, we specialize immediately to the case where y is perpendicular to the direction of motion x , which among other reasons is of particular interest in view of the connection with [21]. The string starts at $r \rightarrow \infty$ and extends down to a minimal radius r_{min} , which by symmetry is such that $Y(r_{min}) = 0$ and $Y'(r_{min}) = \infty$ (which is of course the condition that the projections of the two halves of the string onto the $r - y$ plane can be glued together smoothly).

The main question is whether such a string also trails behind its endpoints and exerts a drag force on them, as would seem compulsory if the string crosses r_v , and

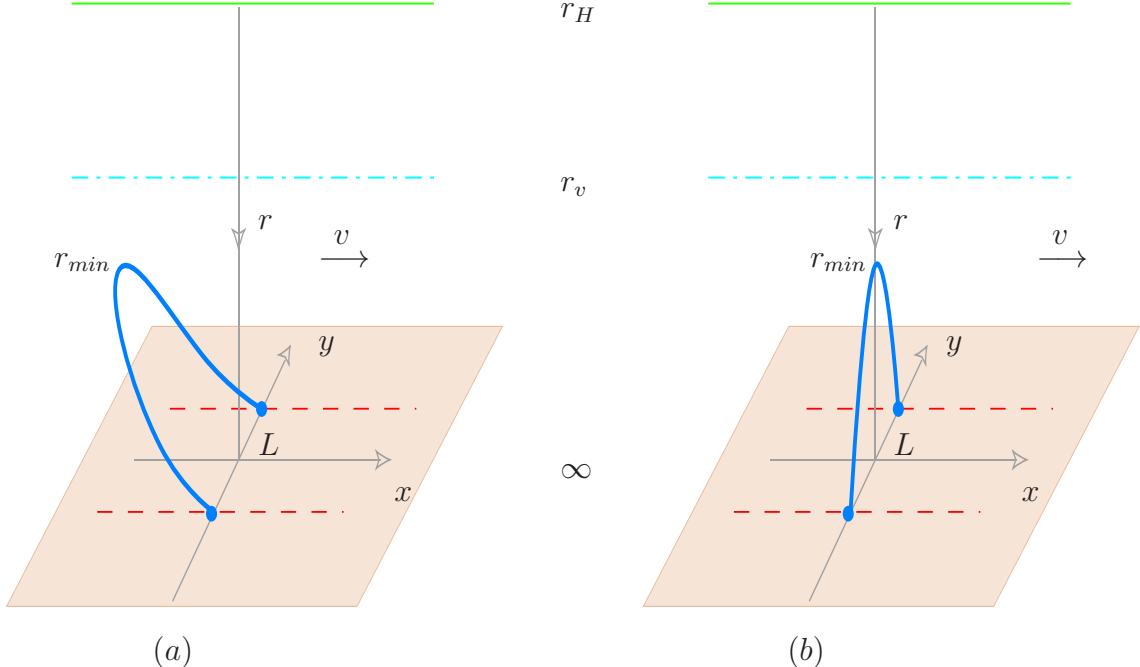


Figure 1: Sketch of the string dual to a moving quark-antiquark pair. The radial coordinate runs downward, so the horizon at $r = r_H$ is shown at the top and the boundary at $r \rightarrow \infty$ is represented by the plane at the bottom. The dash-dot line at $r = r_v$ marks a velocity-dependent radius beyond which the string cannot penetrate. As the string moves to the right, its endpoints (dual to the external quark and antiquark) trace out the dotted trajectories. Its shape codifies information on the configuration of the SYM color fields. (a) One might expect the string to lean backward as a result of the motion. This turns out to be possible only if the string has a nontrivial time-dependence. (b) The lowest-energy configuration for the moving string is in fact upright, similar to the one obtained in the static case. See text for further discussion.

might appear natural more generally on physical grounds. The shape of the string would then be similar to that shown in Fig. 1a. It is easy to see, however, that this cannot happen. The reason is that, on the one hand, the force along the direction of motion must vanish at the midpoint ($r = r_{min}$), because by symmetry the string at that point must be perpendicular to the x -axis, and on the other hand, the force must be constant along the string, because each of its segments moves at constant velocity. We conclude then that $F_x = 0$ everywhere, which implies that the string remains upright, as in Fig. 1b.

Since we initially envisioned the string as being pulled along from its endpoints, it might seem somewhat counterintuitive that it does not lean backward. To clarify this point, it is worth noting that the r -independence of $F_x \propto \Pi_x^r$ is a consequence of the equation of motion for X (or, equivalently, the covariant conservation law for the momentum current P_x^α),

$$\partial_t(\Pi_x^t) + \partial_r(\Pi_x^r) = 0, \quad (12)$$

where the first term vanishes due to the trivial time-dependence of the embedding functions (9) and (10) (while the right-hand side vanishes because \mathcal{L} is independent of X). From this it becomes clear that the conclusion of the previous paragraph can be avoided, and the string can lean backward, if and only if it displays a more complicated time dependence (e.g., some type of oscillatory behavior).

The basic issue here is a familiar one: specifying boundary conditions for the string does not select a unique solution to the corresponding equation of motion; one must additionally specify initial conditions. If the string is initially upright and moving as a whole at velocity v , then as we have seen it will continue to do so, and its endpoints will trace the required paths without requiring an external agent that pulls on them in the direction of motion. On the other hand, if the string is initially static and *then* we start pulling its endpoints with whatever force is necessary for them to move at constant velocity v , the string *will* of course lean backward, as in Fig. 1a. What we have learned above, however, is that such a string will continue to oscillate and will never (classically) stabilize to a configuration of the type (9). The solution in question is therefore clearly not the one with the lowest energy for the given boundary conditions. Nevertheless, as we will see in the next section, there are circumstances under which this type of solution might conceivably play a role in the computation of the energy for the quark-antiquark system of interest to us.

We should similarly keep in mind that it is possible to satisfy the boundary conditions (11) with two *separate* strings that reach all the way down from the boundary to the horizon at fixed $Y = \mp L/2$, trailing behind their endpoints as described in [6, 7]. Such configuration would clearly describe an unbound quark and antiquark, and it will also be of relevance below.

Let us now proceed towards the determination of the shape of the moving string in the AdS-Schwarzschild background. Using the explicit form of the metric²

$$\begin{aligned} ds^2 &= \frac{1}{\sqrt{H}} \left(-h dt^2 + d\vec{x}^2 \right) + \frac{\sqrt{H}}{h} dr^2, \\ H &= \frac{R^4}{r^4}, \quad h = 1 - \frac{r_H^4}{r^4}, \end{aligned} \quad (13)$$

together with the embedding functions (9) and (10), the Lagrangian density (2) simplifies to

$$\mathcal{L} = -\sqrt{-g} = -\sqrt{1 + \frac{h}{H} (X'^2 + Y'^2) - \frac{v^2}{H} Y'^2 - \frac{v^2}{h}}. \quad (14)$$

The associated non-vanishing canonical momentum densities are

$$\begin{aligned} \Pi_t &= \frac{-1}{\sqrt{-g}} \left[1 + \frac{h}{H} (X'^2 + Y'^2) \right], \\ \Pi_x &= \frac{v}{\sqrt{-g}} \left[\frac{1}{h} + \frac{1}{H} Y'^2 \right], \end{aligned}$$

²The relevant background is as usual (AdS-Schwarzschild)₅ × **S**⁵, but we display only the metric for the first factor because the string is taken to lie at a fixed position on the **S**⁵.

$$\begin{aligned}
\Pi_t^r &= \frac{v}{\sqrt{-g}} \left[\frac{h}{H} X' \right], \\
\Pi_x^r &= \frac{-1}{\sqrt{-g}} \left[\frac{h}{H} X' \right], \\
\Pi_y^r &= \frac{-1}{\sqrt{-g}} \left[\frac{h - v^2}{H} Y' \right].
\end{aligned} \tag{15}$$

As already noted above, given that the string moves at constant velocity and \mathcal{L} is independent of X , the corresponding equation of motion (12) is just the statement that the conjugate momentum density Π_x^r is a (real) constant, which we will denote Π_x in what follows. The same is of course true for $\Pi_y \equiv \Pi_y^r$. According to (5), these constants determine the forces $-F_x$ and $-F_y$ that an external agent must exert on the string endpoints to satisfy the given Dirichlet boundary conditions (11). This agent supplies energy to the string at a rate $dE/dt = \Pi_t^r/2\pi\alpha'$, which as expected is seen from (15) to equal the work $-vF_x$.

Inverting the relations (15) to express X' and Y' in terms of the constants Π_x and Π_y , we obtain

$$X' = -\Pi_x \frac{(h - v^2)}{h} \sqrt{\frac{H}{(h - v^2)(\frac{h}{H} - \Pi_x^2) - h\Pi_y^2}}, \tag{16}$$

$$Y' = -\Pi_y \sqrt{\frac{H}{(h - v^2)(\frac{h}{H} - \Pi_x^2) - h\Pi_y^2}}, \tag{17}$$

where we notice the appearance of the same factor $h - v^2$ whose vanishing defined the critical radius (8) that as explained above played a crucial role in fixing the value

$$\Pi_x = -\frac{v}{\sqrt{1 - v^2}} \left(\frac{r_H}{R} \right)^2 \tag{18}$$

for the string dual to a moving quark [6, 7].

There are two immediate things we can learn from the above equations. First, we see from (17) that Y' diverges at the point where the denominator vanishes; according to the characterization following (10) this defines the turnaround point r_{min} :

$$\left[(h - v^2) \left(\frac{1}{H} - \frac{\Pi_x^2}{h} \right) \right]_{r=r_{min}} = \Pi_y^2. \tag{19}$$

It is easy to show from this expression that $r_{min} \geq r_v$, where equality holds only if $\Pi_y = 0$ (which would imply $L = 0$). So, as expected, we find that the string dual to the moving quark-antiquark pair cannot penetrate beyond the critical radius r_v .

Second, in order for the projections of the two halves of the string onto the $y - x$ plane to join smoothly, we must require that $\partial Y/\partial X = Y'/X' = \infty$ at r_{min} , but taking the quotient of (17) and (16) we see that this is *not* possible unless $\Pi_x = 0$, and therefore $X' = 0$. So, as we had already anticipated, we learn that the string can

only move at constant speed if it is upright. This same conclusion has been reached independently in [33].

Specializing (17), (19), (14) and (15) to the case $X' = 0$ ($\Rightarrow \xi(r) = 0$), we can now derive the equations that will be of interest to us in the remainder of this paper. The profile of the upright \cap -shaped string that moves with velocity v and has endpoint separation L is determined by

$$Y' = -\Pi_y \frac{R^4}{\sqrt{(r^4 - r_H^4)(r^4(1 - v^2) - r_H^4 - R^4\Pi_y^2)}} , \quad (20)$$

where the value of Π_y must be chosen in such a way that

$$L = 2 \int_{r_{min}}^{\infty} dr Y' = 2\Pi_y R^4 \int_{r_{min}}^{\infty} \frac{dr}{\sqrt{(r^4 - r_H^4)(r^4(1 - v^2) - r_H^4 - R^4\Pi_y^2)}} , \quad (21)$$

with

$$r_{min} = \left(\frac{r_H^4 + R^4\Pi_y^2}{1 - v^2} \right)^{1/4} . \quad (22)$$

Using (20), the Lagrangian density (14) reduces to

$$\mathcal{L}_{bound} = -\frac{r^4(1 - v^2) - r_H^4}{\sqrt{(r^4 - r_H^4)(r^4(1 - v^2) - r_H^4 - R^4\Pi_y^2)}} . \quad (23)$$

Close to the boundary we find $\mathcal{L}_{bound} \rightarrow -\sqrt{1 - v^2}$, which upon integration implies that the total worldsheet area per unit boundary time is linearly divergent— an obvious consequence of the fact that the string extends all the way to spatial infinity. The same divergence is found in the area of the two disconnected worldsheets dual to the unbound quark and antiquark, described by (14)-(17) with $\Pi_y = 0$ and Π_x as in (18), which result in $\mathcal{L}_{unbound} = -\sqrt{1 - v^2}$. Subtracting the two areas we find the finite expression³

$$A = -\frac{2}{2\pi\alpha'} \int_{-\mathcal{T}/2}^{+\mathcal{T}/2} dt \left(\int_{r_{min}}^{\infty} dr \mathcal{L}_{bound} - \int_{r_H}^{\infty} dr \mathcal{L}_{unbound} \right) . \quad (24)$$

According to the standard recipe [23], in the dual finite-temperature gauge theory, the relative area (24) determines the expectation value (in a stationary phase approximation) of the Wilson loop traced by the moving quark-antiquark pair.

We are also interested in computing the total energy of the \cap -shaped string, which translates into the energy of the quark-antiquark pair. Starting from (15), the Hamiltonian density $\mathcal{H} \equiv -\Pi_t^t$ works out to

$$\mathcal{H}_{bound} = \frac{r^4 - r_H^4}{\sqrt{r^4(1 - v^2) - r_H^4 - R^4\Pi_y^2}} . \quad (25)$$

³In more accurate language, one should as usual introduce a regulating surface at a large radius $r = r_\Lambda$ to make both integrals finite, subtract, and in the end take $r_\Lambda \rightarrow \infty$. In the dual gauge theory, this is equivalent to introducing a UV cutoff $\Lambda \simeq r_\Lambda/R^2$.

As expected, the behavior of this expression near the boundary gives rise to a linear divergence in the total energy of the string, which could again be cancelled by subtracting the energy of the disconnected strings dual to the unbound quark and antiquark, obtained from integrating

$$\mathcal{H}_{unbound} = \frac{r^4 - r_H^4(1 - v^2)}{(r^4 - r_H^4)\sqrt{1 - v^2}}. \quad (26)$$

This subtraction, however, would introduce a new infinity, because (26) implies that the energy of each of the moving unbound strings is logarithmically divergent at the $r = r_H$ endpoint of the integration [6]. The physical origin of this divergence is the infinite amount of energy that has been provided to the system by the external agent that has pulled the boundary endpoint of the string along the x direction for an infinite period of time. From the perspective of a boundary observer, over the course of time this energy has flowed along the string and accumulated in the vicinity of the horizon.

As explained in [6], a simple estimate of the work done on the trailing string by the external agent is obtained by assuming that it has exerted precisely the force needed to overcome the constant drag force (18) over exactly the (infinite) distance that separates the front (boundary) and back (horizon) endpoints of the string. A short calculation shows that this amounts to identifying

$$\mathcal{H}_{unbound}^{input} = \frac{r_H^4 v^2}{(r^4 - r_H^4)\sqrt{1 - v^2}} \quad (27)$$

as the energy density provided by the external agent. Subtracting this from (26), we obtain an estimate of the energy density ‘intrinsic’ to the moving string,

$$\mathcal{H}_{unbound}^{intrinsic} \equiv \mathcal{H}_{unbound} - \mathcal{H}_{unbound}^{input} = \frac{1}{\sqrt{1 - v^2}}, \quad (28)$$

which, as expected, no longer includes the logarithmically-divergent portion. The prescription for eliminating this divergence is of course highly non-unique: one may add to (27) *any* function $\mathcal{U}(r, v)$ such that $U(v) \equiv \int_{r_H}^{\infty} \mathcal{U}(r, v) < \infty$ (in order for \mathcal{U} to represent a finite renormalization of the string energy) and $\mathcal{U}(r, 0) = 0$ (to continue to match the known energy of the static string).

For use below, it is convenient to note here that a completely analogous story applies to the linear momentum $\mathcal{P} \equiv \Pi_x^t$ of the unbound strings [6]: upon integration, the momentum density $\mathcal{P}_{unbound} = v/(h\sqrt{1 - v^2})$ which follows from (15) leads to both a linear divergence at $r \rightarrow \infty$ and a log divergence at $r = r_H$; the latter is a reflection of the infinite amount of momentum provided by the external agent, which can be estimated to be $\mathcal{P}_{unbound}^{input} = \mathcal{H}_{unbound}^{input}/v$; the remaining $\mathcal{P}_{unbound}^{intrinsic} = v/\sqrt{1 - v^2}$ is then an estimate of the momentum density intrinsic to the moving string.

The preceding discussion points towards

$$E \equiv \frac{2}{2\pi\alpha'} \left(\int_{r_{min}}^{\infty} dr \mathcal{H}_{bound} - \int_{r_H}^{\infty} dr \mathcal{H}_{unbound}^{intrinsic} + U(v) \right) \quad (29)$$

as a simple and finite expression that codifies the energy of the moving \cap -shaped string relative to that of the two moving disconnected strings, or, in dual language, the energy of the quark-antiquark pair relative to that of the unbound quark and antiquark. This definition captures, for any given v , the correct L -dependence of the energy of the bound system. The arbitrariness involved in the choice of the function $U(v)$ leads, however, to two important drawbacks: it denies meaning to a direct comparison of values of the energy computed at different velocities, and makes it impossible to deduce from the value of $E(L, v)$ alone whether, for a given L and v , the energetics favor the bound or the unbound configuration. The resolution of these problems will require establishing an unequivocal operational definition of the intrinsic energy of the moving unbound strings (a natural suggestion was made in [6]).

As we have seen, the source of the ambiguity in the definition of $E(L, v)$ is the infinite amount of energy supplied to the unbound strings by the agent that drags them, so a natural way to sidestep this difficulty is to compute the energy in the string rest frame, where the external agent does no work. The requisite coordinate transformation is of course

$$\begin{aligned}\bar{t} &= \gamma(t - vx) , \\ \bar{x} &= \gamma(x - vt) , \\ \bar{y} &= y , \\ \bar{r} &= r ,\end{aligned}\tag{30}$$

(with $\gamma \equiv 1/\sqrt{1 - v^2}$) and amounts, from the gauge theory point of view, to a Lorentz boost that takes us from the rest frame of the plasma, where we had worked up to now, to the rest frame of the quark and antiquark. The canonical momentum densities (15) transform according to

$$\begin{aligned}\bar{\Pi}_{\bar{\mu}}^{\bar{\tau}} &= \frac{\partial X^\nu}{\partial \bar{X}^{\bar{\mu}}} \left(\frac{\partial \sigma}{\partial \bar{\sigma}} \Pi_\nu^\tau - \frac{\partial \tau}{\partial \bar{\sigma}} \Pi_\nu^\sigma \right) , \\ \bar{\Pi}_{\bar{\mu}}^{\bar{\sigma}} &= \frac{\partial X^\nu}{\partial \bar{X}^{\bar{\mu}}} \left(\frac{\partial \tau}{\partial \bar{\tau}} \Pi_\nu^\sigma - \frac{\partial \sigma}{\partial \bar{\tau}} \Pi_\nu^\tau \right) ,\end{aligned}\tag{31}$$

where we have taken into account the effect of the change from the static gauge in the plasma rest frame ($\tau = X^0, \sigma = R$) to the static gauge in the quark rest frame ($\bar{\tau} = \bar{X}^0, \bar{\sigma} = \bar{R}$).

It is easy to check that $\bar{\Pi}_{\bar{t}}^{\bar{\tau}} = 0$, which shows that, as expected, in this frame no energy is being supplied to the string. The total energy of the unbound strings will consequently have no logarithmic divergence, and its linear divergence will serve to cancel that of the \cap -shaped string in the usual straightforward way. Because the string is static, we find $\bar{\mathcal{H}} = -\bar{\Pi}_{\bar{t}}^{\bar{\tau}} = -\bar{\mathcal{L}}$, and from the fact that the Lagrangian transforms as a scalar density it follows that $\bar{\mathcal{L}} = \gamma \mathcal{L}$, so the energy of the bound system relative to that of the unbound system,

$$\bar{E} \equiv -\frac{2}{2\pi\alpha'} \left(\int_{r_{min}}^{\infty} dr \bar{\mathcal{L}}_{bound} - \int_{r_H}^{\infty} dr \bar{\mathcal{L}}_{unbound} \right) ,\tag{32}$$

is related to the area (24) through $\bar{E} = \gamma A/\mathcal{T} = A/\bar{\mathcal{T}}$, just like it should. We stress that in this frame we have been able to cleanly subtract the energy of the unbound strings without introducing any ambiguities, so both the L - and v -dependence of (32) are physically meaningful, and the bound configuration is known to be energetically preferred whenever $\bar{E}(L, v) < 0$.

It is interesting to note that, in contrast with the energy, even in the rest frame the linear momentum of the string *cannot* be defined unequivocally without additional physical input. Even though the external agent does no work on either the bound or unbound strings, in the latter case it does supply momentum to the static string: in gauge theory language, a force must be exerted to hold the isolated quark in place as the plasma flows by at speed v . As a result, the momentum density $\bar{\mathcal{P}}_{unbound} = v\gamma^2(1-h)/h$ for the disconnected strings gives rise to a logarithmic divergence at the $r = r_H$ endpoint of the integration. This may be eliminated by subtracting the estimate

$$\bar{\mathcal{P}}_{unbound}^{input} = v\gamma^2 \left(\frac{1-h}{h} \right) \quad (33)$$

for the momentum supplied by the external agent, which can be obtained either by Lorentz-transforming $(\Pi_\mu^\alpha)_{unbound}^{input}$ to the barred frame, or by recomputing directly in the barred frame under assumptions parallel to those that led to (27). After this subtraction, one would be left with $\bar{\mathcal{P}}_{unbound}^{intrinsic} = 0$ as an estimate of the momentum intrinsically associated with the string. This vanishing result might at first sight appear natural and unambiguous, since the string is, after all, at rest. That the issue is not this simple becomes clear upon observing that the momentum density for the \cap -shaped string,

$$\bar{\mathcal{P}}_{bound} = v\gamma(1-h)\mathcal{H}, \quad (34)$$

is non-vanishing, despite the fact that this string is also at rest, and no external momentum has been supplied to it. This is only possible because in the barred frame $\bar{g}_{\bar{t}\bar{x}} \neq 0$, so the metric is not static. We will come back to this discussion in the next section.

3 Energy of Moving Quark-Antiquark System

In this section we will use the above results for the moving string to make various inferences about the dual system: an external quark-antiquark pair in $SU(N)$ $\mathcal{N} = 4$ SYM with 't Hooft coupling $g_{YM}^2 N$ and temperature T determined by the AdS radius R , horizon radius r_H and string length $\sqrt{\alpha'}$ through [3]

$$g_{YM}^2 N = \frac{R^4}{\alpha'^2}, \quad T = \frac{r_H}{\pi R^2}. \quad (35)$$

According to (5), the fact that $\Pi_x = 0$ translates into the statement that, in stark contrast with the solitary quark considered in [6, 7], an external quark-antiquark

pair feels no drag force as it ploughs through the plasma, a curious result that was obtained independently in the recent paper [33].

As explained in [6, 7] and analyzed more closely in [14, 15, 16], a moving quark produces an extended wake in the color fields, which may be regarded as a coherent spray of gluons radiated away from the quark, and is the CFT dual of the trailing string that extends all the way down to the horizon. It is this wake that transports energy and momentum away from the quark and into the surrounding medium. It is worth noting that this mechanism can operate even at zero temperature, where there is no plasma: given appropriate initial conditions for the gluonic fields, a quark moving at constant speed *can* lose energy to the wake it imprints on these fields. The dual statement is that a string on pure AdS that displays a non-trivial time-dependence *can* trail behind its boundary endpoint even if the latter moves at constant velocity.⁴ This, of course, should not come as a surprise, because the SYM vacuum constitutes, after all, a highly nonlinear polarizable medium. Needless to say, the lowest-energy configuration for the gluonic field profile surrounding the moving quark at zero temperature is the one obtained by boosting the static profile; this configuration is dual to an upright string, which feels no drag force. The string considered in [6, 7] correctly reduces to this case when $T \rightarrow 0$, which ensures that the energy loss process studied there is intrinsically associated with the presence of the plasma.

Unlike the single quark, which carries a net color charge, the quark-antiquark pair is a dipole, and consequently sets up a shorter-ranged profile in the gluonic fields. At zero-temperature, the dipolar $\text{Tr } F^2$ falloff is proportional to L^3/r^7 [18, 35], compared to the Coulomb-like $1/r^4$ of the monopole [17]. At finite temperature, we have learned here that the profile generated by the moving pair is not able to transport energy away from it, a property that could plausibly be verified using the methods of [14, 15, 16]. In the $N \gg 1$, $g_{YM}^2 N \gg 1$ regime of the gauge theory that is captured by classical string theory on weakly-curved AdS-Schwarzschild, no other mechanism of energy loss is at work, and so the quark-antiquark pair moves through the plasma unimpeded. This result should generalize to any color-neutral probe of the plasma, including the baryon, whose static AdS dual was constructed in [36, 37, 38] and whose zero-temperature $\text{Tr } F^2$ falloff is also $\propto r^{-7}$ [18]. The remarks we made above for the solitary quark at $T = 0$ apply as well to these color-neutral systems at $T > 0$: with a different set of initial conditions for the gluonic fields, the quark-antiquark pair and the baryon *can* experience a drag force.

Let us now proceed to determine the energies \bar{E} and E of the quark-antiquark pair for a given velocity v and separation L . For this we first need to carry out the integrals (21), (32) and (29) to find $L(\Pi_y, v)$, $\bar{E}(\Pi_y, v)$ and $E(\Pi_y, v)$, and then eliminate Π_y to obtain $\bar{E}(L, v)$ and $E(L, v)$. As indicated in (3) and explained in the discussion below (15), Π_y is a measure of the force F_y that an external agent must exert in order to keep the $q\bar{q}$ pair at the desired separation.

Unfortunately, the integrals cannot be performed analytically, so we must solve

⁴The assertion for the string may be deduced from an argument similar to the discussion following (12); its SYM dual could be verified through calculations similar to those performed in [18].

the problem numerically. For this purpose, it is convenient to use $h = 1 - r_H^4/r^4$ in place of r as the integration variable. The range of integration should then be taken from

$$h_{min} \equiv h(r_{min}) = \frac{v^2 + f_y^2}{1 + f_y^2} \quad (36)$$

to 1, where we have defined the rescaled force

$$f_y \equiv \frac{R^2}{r_H^2} \Pi_y = \frac{2}{\pi \sqrt{g_{YM}^2 N T^2}} F_y .$$

The result $r_{min} > r_v$ of the previous section translates into $h_{min} > v^2$, which can also be easily deduced from (36). After changing variables in this manner and using the dictionary (35), the expression for the quark-antiquark separation (21) turns into

$$L(f_y, v) = \frac{f_y}{2\pi T} \int_{h_{min}}^1 \frac{dh}{(1-h)^{\frac{1}{4}} \sqrt{(h-v^2)h - (1-h)hf_y^2}} , \quad (37)$$

and the energy of the $q\bar{q}$ pair in its rest frame (32) becomes⁵

$$\bar{E}(f_y, v) = \frac{T\sqrt{g_{YM}^2 N}}{4} \left[\int_{h_{min}}^1 \frac{dh(h-v^2)\gamma}{(1-h)^{\frac{5}{4}} \sqrt{(h-v^2)h - (1-h)hf_y^2}} - \int_0^1 \frac{dh}{(1-h)^{\frac{5}{4}}} \right] . \quad (38)$$

As noted at the end of the previous section, the subtraction implemented by the second term in equation (38) ensures a finite result and corresponds to removing the self-energies of the quark and antiquark separately held in place as the plasma flows by with velocity v in the $-x$ direction. The energy of the system in the frame where the plasma is static and the pair moves is given instead by (29), which translates into

$$E(f_y, v) - U(v) = \frac{T\sqrt{g_{YM}^2 N}}{4} \left[\int_{h_{min}}^1 \frac{dh\sqrt{h}}{(1-h)^{\frac{5}{4}} \sqrt{(h-v^2)h - (1-h)hf_y^2}} - \int_0^1 \frac{dh\gamma}{(1-h)^{\frac{5}{4}}} \right] . \quad (39)$$

As explained below (28), the function $U(v)$ reflects an ambiguity in separating the energy intrinsically associated with the moving quark from the energy supplied by the agent that pulls the quark and lost to the plasma.

Notice that while the second terms in the plasma frame energy (39) and the $q\bar{q}$ frame energy (38) are proportional to one another, the first terms are not. The reason is that the boost that takes us back from the $q\bar{q}$ frame to the plasma frame mixes the energy $\int_{h_{min}}^1 dh \bar{\mathcal{H}}_{bound}$ of the pair with its momentum $\int_{h_{min}}^1 dh \bar{\mathcal{P}}_{bound}$, which as seen in (34) is non-vanishing. Since by definition the quark and antiquark are at rest in this frame, it is clear that the momentum in question is carried not directly by them,

⁵An overall factor of γ was missing from the energies computed in the first version of this paper that was posted on the arXiv. We thank Hong Liu for bringing this to our attention.

but by the gluonic field configuration produced by their interaction with the flowing plasma, i.e., the momentum density $\bar{\mathcal{P}}(r)$ encodes the chromodynamic analog of the electromagnetic Poynting vector, at the energy scale $\sim r/R^2$.⁶ It would be interesting to explore this relation in more detail using the methods of [16].

Even though (38) and (39) are not proportional to one another, they turn out to be related through the relatively simple expression

$$E(L, v) - U(v) = \gamma \bar{E}(L, v) + \frac{\pi}{2} \sqrt{g_{YM}^2 N T^2} \frac{v^2 \gamma^2 L}{f_y}. \quad (40)$$

This enables one to determine $E(L, v)$ once $\bar{E}(L, v)$ is known, without having to carry out any additional numerical integration, so in the remainder of this paper we will concentrate on computing the latter.

The results of the numerical integration of (37) are shown in Fig. 2, which displays

$$l \equiv 2\pi T L$$

as a function of the applied external force f_y for a few different values of v . The behavior is in all cases qualitatively the same as was found in [31, 32] for the static case: at any given v , it is only possible to attain separations in a finite range $0 \leq L \leq L_{max}(v)$, and each separation in this range can be achieved with two different values of the force F_y . The exception is of course the maximum $L_{max}(v)$, whose physical meaning will become clear below, and which we find empirically to be located at a value of the external force that can be well-approximated with a quadratic function of the velocity,

$$f_{y,max}(v) \simeq 0.949 + 0.247v + 0.223v^2. \quad (41)$$

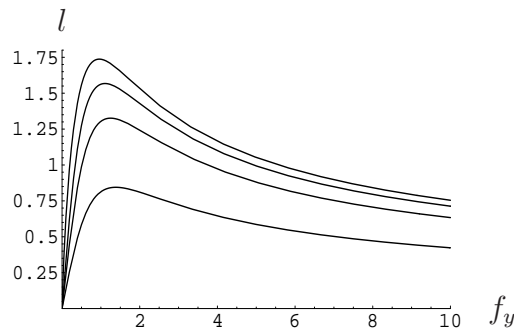


Figure 2: Quark-antiquark separation (in units of $1/2\pi T$) as a function of the applied external force (in units of $\pi\sqrt{g_{YM}^2 NT^2}/2$), for velocities $v = 0, 0.45, 0.7, 0.95$. Lower curves correspond to larger velocities.

⁶This also leads one to expect the momentum intrinsic to the isolated quark held fixed in the flowing plasma to be non-vanishing, unlike what the naive estimate (33) (which corresponds to $U(v) = 0$) would have indicated.

Combining these results with the numerical integration of (38), we can find the quark-antiquark energy $\bar{E}(L, v)$ for any velocity $0 \leq v \leq 1$ and separation $0 \leq L \leq L_{max}(v)$. The results are plotted in Figs. 3 and 4, which display

$$\bar{e} \equiv \frac{4}{\sqrt{g_{YM}^2 N T}} \bar{E}$$

as a function of l , for a few representative values of v . In each case the curve is divided into two parts: a dashed portion obtained from the smaller value of the applied force consistent with the given separation L (i.e., $f_y < f_{y_{max}}$), and a solid portion obtained from the larger value ($f_y \geq f_{y_{max}}$). As we can see in the figures, it is this latter case that gives the lower value for the quark-antiquark energy, and consequently the solid curve describes the stable configurations that are of most interest to us. The dashed curve is associated instead with configurations that are physical and can be selected through a proper choice of initial conditions for the gluonic fields in SYM (or, in dual language, for the string in AdS-Schwarzschild), but are only metastable (i.e., they are stable under small, but not arbitrary, fluctuations).

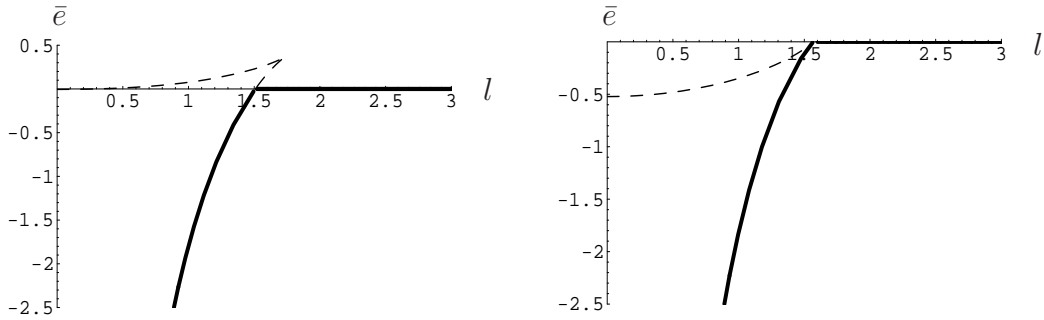


Figure 3: Quark-antiquark energy (in units of $T\sqrt{g_{YM}^2 N}/4$) as a function of separation (in units of $1/2\pi T$), for (a) $v = 0$ (b) $v = 0.45$. The solid (dashed) portion of each curve corresponds to stable (metastable) configurations.

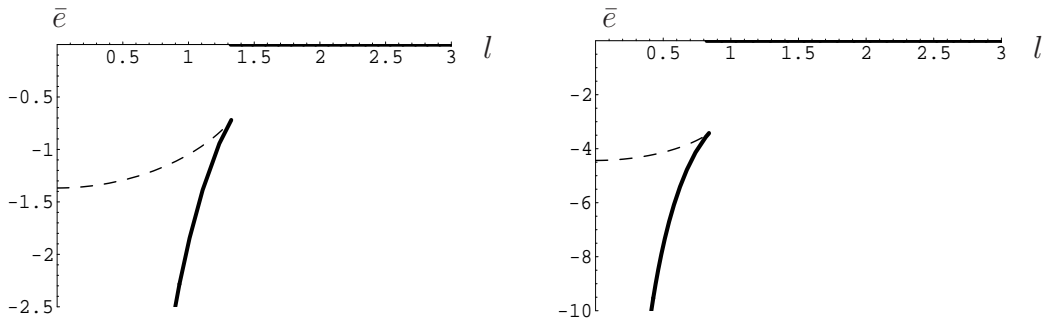


Figure 4: Quark-antiquark energy (in units of $T\sqrt{g_{YM}^2 N}/4$) as a function of separation (in units of $1/2\pi T$), for (a) $v = 0.7$, (b) $v = 0.95$. The solid (dashed) portion of each curve corresponds to stable (metastable) configurations.

In Fig. 3a we verify that for the static configuration $v = 0$ we correctly reproduce the $q\bar{q}$ potential computed in [31, 32], which, as explained there, encodes all of the expected physics. At small separations (large energies) the quark-antiquark pair becomes insensitive to the plasma and as a result the potential approaches the $1/L$ behavior obtained at $T = 0$ in [23]. As the separation grows, however, the effects of the plasma progressively screen the quark and antiquark from one another, and as a consequence raise the system's energy above the Coulombic behavior. The screening becomes complete at the distance $L_* \approx 1.51/2\pi T < L_{max}(0)$ where the energy matches that of the unbound system. For separations larger than this screening length, the quark and antiquark are free and the $q\bar{q}$ potential vanishes, as indicated by the horizontal solid line. The configurations described by (37) and (38) in the range $L_* < L \leq L_{max}$ are only metastable, which is why the corresponding portion of the curve is also dashed.

As seen in Figs. 3 and 4, the results for $v > 0$ have many similarities with the static case. The main overall effect of increasing the velocity is to move the $\bar{E}(L)$ curve to the left and down. The dependence of L_{max} on the velocity is given by the solid line in Fig. 5. We find it to be quite close to

$$L_{max}(v) \simeq \frac{1.73}{2\pi T}(1 - v^2)^{1/3} , \quad (42)$$

shown as the long-dash line in the figure. We will comment on the precise $v \rightarrow 1$ behavior below.

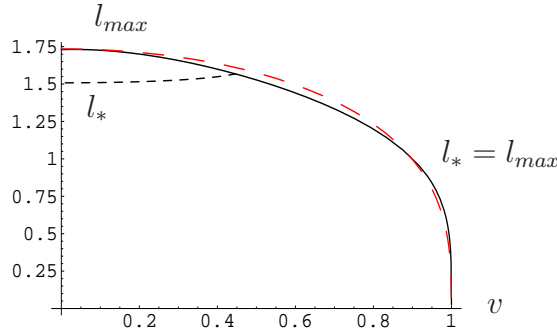


Figure 5: Maximum quark-antiquark distance L_{max} and screening length L_* as functions of the velocity. Both lengths are given in units of $1/2\pi T$.

The energy at this maximum separation, $\bar{E}_{max}(v) \equiv \bar{E}(L_{max}, v)$ is shown as a function of velocity in Fig. 6. For increasing v this energy decreases, passing through zero at a velocity ~ 0.447 , and then approaching $-\infty$ as $v \rightarrow 1$. We find that over most of the $0 \leq v \leq 1$ range the graph is practically indistinguishable from that of the function

$$\bar{E}_{max}(v) \simeq \frac{0.368T\sqrt{g_{YM}^2 N}}{4}(1 - 5v^2)(1 - v^2)^{-5/12} . \quad (43)$$

The precise behavior in the $v \rightarrow 1$ limit will be determined below.

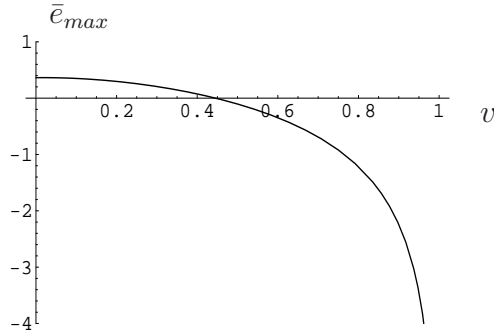


Figure 6: Maximum energy as a function of v , in units of $T\sqrt{g_{YM}^2 N}/4$.

For any velocity, we expect the presence of the plasma to become irrelevant at short distances, so at small L our results should approach the corresponding zero-temperature curves. The latter can be determined analytically. By taking the $T \rightarrow 0$ limit in (37), (38) and (22) we obtain

$$L = 2R^4\Pi_y \int_{r_{min}}^{\infty} \frac{dr}{r^2\sqrt{(1-v^2)r^4 - R^4\Pi_y^2}} \quad (44)$$

and

$$\bar{E} = \frac{1}{\pi\alpha'} \left[\int_{r_{min}}^{\infty} \frac{r^2\sqrt{1-v^2}dr}{\sqrt{(1-v^2)r^4 - R^4\Pi_y^2}} - \int_0^{\infty} dr \right], \quad (45)$$

with $r_{min} = R\sqrt{\Pi_y}/(1-v^2)^{1/4}$. Changing to the dimensionless integration variable $\rho \equiv (1-v^2)^{1/4}r/R\sqrt{\Pi_y}$, it is possible to find an explicit relation between \bar{E} and L ,

$$\bar{E}(L, v) = -\frac{4\pi^2\sqrt{g_{YM}^2 N}}{\Gamma(\frac{1}{4})^4 L}, \quad (46)$$

which agrees for any v with the static result obtained some years ago in [23]. We have checked that our results for $\bar{E}(L, v)$ at finite temperature correctly approach (46) at small separation. The reason for this agreement is evident from the string theory side: the limit $L \rightarrow 0$ implies that $r_{min} \rightarrow \infty$, so for small separations the string does not penetrate far into the AdS-Schwarzschild geometry, and it is difficult for it to sense the difference with pure AdS. Notice also that, in this limit, the second term in both the left- and right-hand side of (40) becomes irrelevant (the former, because the ambiguity that led to $U(v)$ was associated with the presence of the horizon; the latter, because it scales like L^3 in this limit), so the plasma frame energy reduces unequivocally to

$$E(L, v) = \gamma\bar{E}(L, v) = -\frac{4\pi^2\sqrt{g_{YM}^2 N}}{\Gamma(\frac{1}{4})^4\sqrt{1-v^2}L}, \quad (47)$$

as dictated by the restored Lorentz invariance.⁷

The behavior of the full $\bar{E}(L, v)$ graph for small velocities is essentially the same as in the static case. As the velocity increases, the screening length $L_*(v)$ (which we always define as the separation beyond which the quark and antiquark become unbound⁸ is found to increase slowly, as shown by the short-dash line in Fig. 5. The dependence is nearly quadratic,

$$L_*(v) \simeq \frac{1.51}{2\pi T} \left(1 + \frac{1}{3}v^2\right) \quad \text{for } v < 0.447. \quad (48)$$

As seen in the same figure, $L_{max}(v)$ is monotonically decreasing, so there is a velocity $v_{gap} \sim 0.447$ at which both lengths coincide; this is precisely the zero in Fig. 6, and explains the bound on the region of validity of (48).

For $v > v_{gap}$, both types of bound solutions (stable and metastable) have negative energy, so a gap begins to develop between the bound and unbound configurations, whose width evolves as indicated in the negative portion of the graph in Fig. 6. Since the width increases without bound as $v \rightarrow 1$, it is natural to wonder whether at $v > v_{gap}$ there could be additional *bound* $q\bar{q}$ configurations which cover a range of separations $L > L_{max}$, and consequently narrow or perhaps even eliminate the gap. As discussed earlier in this section, there certainly exist configurations in which the quark and antiquark move at constant velocity but the color fields display a more complicated time dependence. Their AdS description was discussed in the paragraphs that follow (12); it involves a string that leans back as in Fig. 1a and has time dependence beyond the overall motion at velocity v . These configurations exist both for $L \leq L_{max}$ and $L > L_{max}$, but in the former case they are clearly metastable and therefore not of interest for the present discussion. What is not at all obvious to us is whether at least one of the configurations for $L > L_{max}$ manages to have negative energy. This is a complicated question that would appear to require numerical exploration of the space of solutions to the corresponding coupled partial differential equations.

In the remainder of this paper we assume that for all values of L and v , the lowest energy configurations are always the ones with the simplest time dependence: for $L < L_{max}$, the bound $q\bar{q}$ system dual to the upright string in Fig. 1b; for $L > L_{max}$, the unbound quark and antiquark dual to two separate copies of the string analyzed in [6, 7]. The graphs in Figs. 3,4 can then be taken at face value, and imply in particular

⁷This dependence was also noted recently in [13], which includes some comments on the finite-temperature behavior of $E(L, v)$ in the ladder approximation of the gauge theory.

⁸Given the shape of the energy graphs, the fact that $\bar{E}(L_*(v), v) = 0$ implies that for separations $L > L_*$ the decay from the bound to the unbound configurations is allowed from the point of view of energy conservation. Since, as we have seen above, the momenta of the configurations is in general non-vanishing (despite the fact that we are in their rest frame), strictly speaking one would also need to check that the decay is allowed from the point of view of momentum conservation. This, however, would require precise knowledge of the momentum intrinsic to the isolated quark, which is at present lacking. Such knowledge would also enable one to determine the screening length directly from the plasma frame energy $E(L, v)$.

that for $v > v_{gap}$ the screening length should be identified with the location of the discontinuity in $\bar{E}(L)$, i.e.,

$$L_*(v) = L_{max}(v) \quad \text{for } v > 0.447. \quad (49)$$

The AdS/CFT prediction for the velocity-dependence of the screening length (for an arbitrary angle θ between the direction of motion and the $q\bar{q}$ separation L) was the main subject of [34],⁹ which appeared while the first version of this paper was in preparation. The authors of that work did not compute $\bar{E}(L, v)$, and chose to define the screening length not as L_* but as the maximum allowed separation L_{max} , throughout the entire range of velocities. Their equations and numerical results (for $\theta = \pi/2$) are in complete agreement with ours. As noted in (42), we have found that, *over the entire range* $0 \leq v \leq 1$, the $L_{max}(v)$ curve is best described as being proportional to $(1 - v^2)^{1/3}$. The authors of [34], on the other hand, have found analytically that the behavior of $L_{max}(v)$ *in the ultra-relativistic limit*¹⁰ is precisely proportional to $(1 - v^2)^{1/4}$. This result can be confirmed directly from (37), which in the $v \rightarrow 1$ limit reduces to

$$L(f_y, v) = \frac{1}{2\pi T} \frac{4\sqrt{2}\pi^{3/2}}{\Gamma(1/4)^2} \frac{f_y}{(1 + f_y^2)^{3/4}} (1 - v^2)^{1/4}. \quad (50)$$

In agreement with (41), this expression has a maximum at $f_{y_{max}} = \sqrt{2}$, which leads to

$$L_{max}(v) = \frac{1}{2\pi T} \frac{3^{-3/4} 8\pi^{3/2}}{\Gamma(1/4)^2} (1 - v^2)^{1/4} \approx \frac{1.49}{2\pi T} (1 - v^2)^{1/4} \quad \text{for } v \sim 1. \quad (51)$$

Combining this with (48) and (49), we obtain the relatively simple expression

$$L_*(v) \simeq \frac{1.51}{2\pi T} \left(1 + \frac{7}{12}v^2 - \frac{7}{12}v^4 \right) (1 - v^2)^{1/4} \quad \text{for } 0 \leq v \leq 1, \quad (52)$$

which captures the correct analytic behavior at $v \rightarrow 0$ and $v \rightarrow 1$, and gives good numerical agreement over the entire range of velocities.

As seen in these last two equations, for large velocities the screening length $L_*(v)$ decreases monotonically to zero, implying that $\bar{E}(L, v) = 0$ everywhere except in the rapidly shrinking range $0 < L < L_*(v)$, where $\bar{E}(L, v)$ may be obtained from (50) and the $v \rightarrow 1$ limit of (38),

$$\bar{E}(f_y, v) = -\frac{T\sqrt{g_{YM}^2 N}}{4} \frac{4\sqrt{2}\pi^{3/2}}{\Gamma(1/4)^2} \frac{2 + f_y^2}{(1 + f_y^2)^{3/4}} (1 - v^2)^{-1/4}. \quad (53)$$

It is interesting to note that even though L is small and the condition $r_{min} > r_v = r_H(1 - v^2)^{-1/4}$ forces the string to stay close to the boundary, the L -dependence of

⁹This work also emphasized the importance of this calculation for advancing towards a quantitative understanding of the J/ψ suppression observed in the quark-gluon plasma produced at RHIC.

¹⁰We thank Hong Liu for clarifying this point to us after the first version of this paper was posted on the arXiv.

the energy remains more complicated than in the $T = 0$ case, and is qualitatively similar to the graphs shown in Fig. 4: there is a metastable region at $f_y < \sqrt{2}$, and a stable region at $f_y > \sqrt{2}$, such that for $f_y \gg 1$ one recovers the Coulombic behavior (46). By evaluating (4) at $f_{y_{max}} = \sqrt{2}$ we find

$$\bar{E}_{max}(v) = -\frac{T\sqrt{g_{YM}^2 N} 2^{9/2} 3^{-3/4} \pi^{3/2}}{4 \Gamma(1/4)^2} (1 - v^2)^{-1/4} \quad \text{for } v \sim 1. \quad (54)$$

Note again the difference in the exponents found here and in (43), which was meant as a fit of $\bar{E}_{max}(v)$ throughout the entire interval $0 \leq v < 1$.

In the $v \rightarrow 1$ limit the Wilson loop traced by our moving quark-antiquark pair approaches the lightlike loop used in [21] to propose a non-perturbative definition of the jet-quenching parameter \hat{q} .¹¹ We would have therefore expected our results to make contact with those of [21] in this limit, and were surprised to find that this is not the case. The difference is drastic: whereas the string of [21] extends all the way from the boundary to the horizon and back, in the $v \rightarrow 1$ limit the string that we use to describe bound configurations explores only an ever-shrinking region of the geometry close to the boundary.¹²

The main obstruction to a continuous interpolation between our results and those of [21] is the fact that for any value of v we have found and employed string worldsheets whose area is real, whereas the authors of [21] work with a worldsheet whose area is imaginary. The difference does not appear to be attributable to the fact that their Wilson loop is strictly lightlike, while ours is (in general) only approximately so, because the gauge theory calculations which motivate the connection to the jet-quenching parameter build upon an eikonal approximation justified in terms of a high energy limit which manifestly takes $v \rightarrow 1$ from below [20, 40]. Moreover, an argument has recently been given in [34, 39] to the effect that the result for the lightlike Wilson loop of [21] can be obtained continuously from Wilson loops that correspond to velocities that approach $v = 1$ from below. The key point is that, for any given $v < 1$, the authors of [21, 34] enforce boundary conditions for the string not at the AdS-Schwarzschild boundary, but at a finite radius $r = r_{LRW} \ll r_v$ (with r_v the critical radius given in (8)). As a result of this, their worldsheet lies entirely in the region $r < r_v$, which is inaccessible to a string that reaches the boundary, as do the strings considered in the present paper. This explains why the worldsheets that lead to the result of [21] are spacelike.

Regrettably, we do not understand the physics behind this prescription. One can envision of course situations where the choice of boundary conditions for a path integral result in its being dominated by a saddle point with imaginary action,¹³ but

¹¹To be more precise, one should take $v \rightarrow -1$ to agree with the conventions of [21].

¹²One should of course remember that such strings are allowed only for separations smaller than the screening length, which approaches zero in the high-velocity limit. For larger separations the system is unbound, and involves two separate strings which do extend from the boundary to the horizon, but are still quite distinct from the string considered in [21].

¹³A simple example is provided by the computation of the propagator for a free relativistic particle moving across a spacelike interval.

we do not see why this should be the case in the problem at hand. To determine the value of a Wilson loop traced by a $q\bar{q}$ pair that moves at any velocity smaller than, but *arbitrarily close* to, the speed of light, the AdS/CFT recipe [23] requires the string boundary conditions (11) to be enforced at $r \rightarrow \infty$, because it is only in this limit that the dual quark and antiquark become pointlike. Since this limit is taken at fixed v , the string in question will have no choice but to lie entirely in the $r > r_v$ region, so its worldsheet will be timelike, and the predicted value for the Wilson loop at strong coupling will unambiguously coincide with the result $\exp[i\bar{\mathcal{T}}\bar{E}(L, v)]$ obtained in this paper.

If the string boundary conditions (11) are enforced instead as advocated in [21, 34, 39], the string endpoints lie at a finite radius $r = r_{LRW} \ll r_v$. In this case the path integral for the string is indeed dominated by a saddle point with imaginary action, a condition which has been argued [34, 39, 40] to be necessary in order to make contact with the jet-quenching parameter defined in phenomenological models of energy loss. But by the standard UV/IR reasoning [41], this path integral would appear to be computing not a standard but a ‘thick’ Wilson loop, traced by sources for the gluonic field that have a characteristic size $d \sim R^2/r_{LRW} \gg R^2/r_v \simeq (1 - v^2)^{1/4}/T$, which according to (52) happens to be much larger than the screening length at the given v . It is unclear to us whether this ‘thick’ loop is in some way relevant to the approximate gauge theory calculations [20] that motivated the proposal of [21]. One should not of course lose sight of the fact that the loop becomes ‘thinner’ (in the sense that $d \rightarrow 0$) as $v \rightarrow 1$, so precisely at $v = 1$ one is computing a standard Wilson loop (with a string worldsheet that correctly extends all the way to the AdS-Schwarzschild boundary). But, as already noted above, the gauge theory basis for the definition of [21] would appear to allow a smooth approach via *standard* Wilson loops with $v \rightarrow 1$ from below, which the AdS/CFT correspondence would compute using timelike worldsheets up to and including $v = 1$ (where we would find $\bar{E}(L, v = 1) = 0$). Perhaps a more useful characterization of the $v = 1$ Wilson loop computed in [21] is as a smooth limit of standard Wilson loops with $v \rightarrow 1$ from *above*.

Before leaving this subject, it is interesting to note that the $\bar{E} \propto L^2$ dependence that was called for in the definition of \hat{q} proposed in [21]— a dependence that was successfully obtained in that work using the spacelike worldsheets discussed in the preceding paragraphs— can also be coaxed out of the $v \rightarrow 1$ limit of the *time-like* worldsheets analyzed in this paper, by focusing not on the stable but on the metastable (dashed) portion of the $\bar{E}(L, v)$ curves of Fig. 4 that lie near the intersection with the \bar{E} axis. This region corresponds to configurations with small separations and small applied external forces, $f_y \ll 1$. Using this condition it is straightforward to infer from (37) and (38) and that, at next-to-leading order in L ,

$$\begin{aligned} \bar{E}(L) = & \frac{T(g_{YM}^2 N)^{\frac{1}{2}}}{4} \left[\int_{h_{min}}^1 \frac{\gamma \sqrt{h - v^2} dh}{\sqrt{h}(1 - h)^{\frac{5}{4}}} - \int_0^1 \frac{dh}{(1 - h)^{\frac{5}{4}}} \right] \\ & + \frac{L^2 T^3 \pi^2 (g_{YM}^2 N)^{\frac{1}{2}}}{2} \gamma \left[\int_{h_{min}}^1 \frac{dh}{(1 - h)^{\frac{1}{4}} \sqrt{h(h - v^2)}} \right]^{-1}, \end{aligned} \quad (55)$$

i.e., the energy depends quadratically on the $q\bar{q}$ separation, as desired. In the limit $v \rightarrow 1$, this relation implies

$$\begin{aligned}\bar{E}(L) &= \frac{\sqrt{2}}{4} \left[-(1-v^2)^{-1/4} \mathcal{A} + (1-v^2)^{-3/4} \mathcal{K} L^2 \right] , \\ \mathcal{A} &= \frac{8\pi^{3/2}}{\Gamma(1/4)^2} \sqrt{g_{YM}^2 N T} , \quad \mathcal{K} = \frac{\sqrt{\pi}}{4} \Gamma(1/4)^2 \sqrt{g_{YM}^2 N T^3} ,\end{aligned}\tag{56}$$

where the numerical prefactor in the first equation has been chosen according to the normalization used in [21], in order to make \mathcal{K} directly comparable to \hat{q} . Independently of whether or not there exists some argument relating the coefficient \mathcal{K} to the jet-quenching parameter as defined in phenomenological models [19, 20], this calculation shows that the information encoded in the parameter \hat{q} defined in [21] can also be accessed using the timelike worldsheets studied in the present paper. This is especially interesting in view of the fact that in the $v \rightarrow 1$ limit, such worldsheets never wander far from the AdS-Schwarzschild boundary. Due to the conformal invariance of the underlying gauge theory, the temperature-dependence of the parameters \mathcal{K} and \hat{q} was bound to agree. The agreement in their 't Hooft-coupling dependence is also not particularly surprising. What is perhaps worth noting is that the numerical coefficients are practically equal,

$$\mathcal{K} = (\Gamma(1/4)^4/16\pi^2)\hat{q} \approx 1.1\hat{q}.$$

In the absence of a direct gauge (or string) theory link between these two parameters, it might be worth exploring their relation in other gauge theories with known gravity duals.

Acknowledgements

It is a pleasure to thank Elena Cáceres for collaboration in the initial stages of this work, for valuable discussions, and for useful comments on the manuscript. We are also grateful to Chris Herzog, Hong Liu, Krishna Rajagopal and Urs Wiedemann for helpful correspondence, and to David Vergara for pointing out a number of relevant references. This work was partially supported by Mexico's National Council of Science and Technology (CONACyT) grants CONACyT 40754-F and CONACyT SEP-2004-C01-47211, as well as by DGAPA-UNAM grant IN104503-3.

References

- [1] J. M. Maldacena, "The large N limit of superconformal field theories and supergravity," *Adv. Theor. Math. Phys.* **2**, 231 (1998) [*Int. J. Theor. Phys.* **38**, 1113 (1999)] [arXiv:hep-th/9711200].

- [2] S. S. Gubser, I. R. Klebanov and A. M. Polyakov, “Gauge theory correlators from non-critical string theory,” *Phys. Lett. B* **428**, 105 (1998) [arXiv:hep-th/9802109];
E. Witten, “Anti-de Sitter space and holography,” *Adv. Theor. Math. Phys.* **2**, 253 (1998) [arXiv:hep-th/9802150].
- [3] O. Aharony, S. S. Gubser, J. M. Maldacena, H. Ooguri and Y. Oz, “Large N field theories, string theory and gravity,” *Phys. Rept.* **323**, 183 (2000) [arXiv:hep-th/9905111].
- [4] K. Adcox *et al.* [PHENIX Collaboration], “Formation of dense partonic matter in relativistic nucleus nucleus collisions at RHIC: Experimental evaluation by the PHENIX collaboration,” *Nucl. Phys. A* **757**, 184 (2005) [arXiv:nucl-ex/0410003];
I. Arsene *et al.* [BRAHMS Collaboration], “Quark gluon plasma and color glass condensate at RHIC? The perspective from the BRAHMS experiment,” *Nucl. Phys. A* **757** (2005) 1 [arXiv:nucl-ex/0410020];
B. B. Back *et al.*, “The PHOBOS perspective on discoveries at RHIC,” *Nucl. Phys. A* **757** (2005) 28 [arXiv:nucl-ex/0410022];
J. Adams *et al.* [STAR Collaboration], “Experimental and theoretical challenges in the search for the quark gluon plasma: The STAR collaboration’s critical assessment of the evidence from RHIC collisions,” *Nucl. Phys. A* **757**, 102 (2005) [arXiv:nucl-ex/0501009].
- [5] F. Carminati *et al.* [ALICE Collaboration], “ALICE: Physics performance report, volume I,” *J. Phys. G* **30** (2004) 1517;
A. Morsch [ALICE Collaboration], “Jet quenching studies with the ALICE detector,” *Czech. J. Phys.* **55** (2005) B333.
- [6] C. P. Herzog, A. Karch, P. Kovtun, C. Kozcaz and L. G. Yaffe, “Energy loss of a heavy quark moving through $N = 4$ supersymmetric Yang-Mills plasma,” arXiv:hep-th/0605158.
- [7] S. S. Gubser, “Drag force in AdS/CFT,” arXiv:hep-th/0605182.
- [8] J. Casalderrey-Solana and D. Teaney, “Heavy quark diffusion in strongly coupled $N = 4$ Yang Mills,” arXiv:hep-ph/0605199.
- [9] C. P. Herzog, “Energy Loss of Heavy Quarks from Asymptotically AdS Geometries,” arXiv:hep-th/0605191.
- [10] E. Cáceres and A. Güijosa, “Drag Force in a Charged $N = 4$ SYM Plasma,” arXiv:hep-th/0605235.
- [11] E. Cáceres and A. Güijosa, “On drag forces and jet quenching in strongly coupled plasmas,” arXiv:hep-th/0606134.

- [12] P. M. Chesler and A. Vuorinen, “Heavy flavor diffusion in weakly coupled N=4 Super Yang-Mills theory,” arXiv:hep-ph/0607148.
- [13] S. J. Sin and I. Zahed, “Ampere’s law and energy loss in AdS/CFT duality,” arXiv:hep-ph/0606049.
- [14] J. J. Friess, S. S. Gubser and G. Michalogiorgakis, “Dissipation from a heavy quark moving through N = 4 super-Yang-Mills plasma,” arXiv:hep-th/0605292.
- [15] Y. h. Gao, W. s. Xu and D. f. Zeng, “Wake of color fields in charged N = 4 SYM plasmas,” arXiv:hep-th/0606266.
- [16] J. J. Friess, S. S. Gubser, G. Michalogiorgakis and S. S. Pufu, “The stress tensor of a quark moving through N=4 thermal plasma,” arXiv:hep-th/0607022.
- [17] U. H. Danielsson, E. Keski-Vakkuri and M. Kruczenski, “Vacua, propagators, and holographic probes in AdS/CFT,” JHEP **9901**, 002 (1999) [arXiv:hep-th/9812007].
- [18] C. G. Callan and A. Güijosa, “Undulating strings and gauge theory waves,” Nucl. Phys. B **565**, 157 (2000) [arXiv:hep-th/9906153].
- [19] R. Baier, D. Schiff and B. G. Zakharov, “Energy loss in perturbative QCD,” Ann. Rev. Nucl. Part. Sci. **50** (2000) 37 [arXiv:hep-ph/0002198];
R. Baier, “Jet quenching,” Nucl. Phys. A **715**, 209 (2003) [arXiv:hep-ph/0209038].
- [20] A. Kovner and U. A. Wiedemann, “Gluon radiation and parton energy loss,” arXiv:hep-ph/0304151.
- [21] H. Liu, K. Rajagopal and U. A. Wiedemann, “Calculating the jet quenching parameter from AdS/CFT,” arXiv:hep-ph/0605178.
- [22] J. Gomis and F. Passerini, “Holographic Wilson loops,” arXiv:hep-th/0604007.
- [23] J. M. Maldacena, “Wilson loops in large N field theories,” Phys. Rev. Lett. **80** (1998) 4859 [arXiv:hep-th/9803002];
S. J. Rey and J. T. Yee, “Macroscopic strings as heavy quarks in large N gauge theory and anti-de Sitter supergravity,” Eur. Phys. J. C **22** (2001) 379 [arXiv:hep-th/9803001].
- [24] A. Buchel, “On jet quenching parameters in strongly coupled non-conformal gauge theories,” arXiv:hep-th/0605178.
- [25] J. F. Vazquez-Poritz, “Enhancing the jet quenching parameter from marginal deformations,” arXiv:hep-th/0605296.

- [26] S. J. Sin and I. Zahed, “Holography of radiation and jet quenching,” *Phys. Lett. B* **608** (2005) 265 [arXiv:hep-th/0407215]
- [27] E. Shuryak, S. J. Sin and I. Zahed, “A gravity dual of RHIC collisions,” arXiv:hep-th/0511199.
- [28] F. L. Lin and T. Matsuo, “Jet quenching parameter in medium with chemical potential from AdS/CFT,” arXiv:hep-th/0606136.
- [29] S. D. Avramis and K. Sfetsos, “Supergravity and the jet quenching parameter in the presence of R-charge densities,” arXiv:hep-th/0606190.
- [30] N. Armesto, J. D. Edelstein and J. Mas, “Jet quenching at finite ’t Hooft coupling and chemical potential from AdS/CFT,” arXiv:hep-ph/0606245.
- [31] S. J. Rey, S. Theisen and J. T. Yee, “Wilson-Polyakov loop at finite temperature in large N gauge theory and anti-de Sitter supergravity,” *Nucl. Phys. B* **527** (1998) 171 [arXiv:hep-th/9803135].
- [32] A. Brandhuber, N. Itzhaki, J. Sonnenschein and S. Yankielowicz, “Wilson loops in the large N limit at finite temperature,” *Phys. Lett. B* **434**, 36 (1998) [arXiv:hep-th/9803137].
- [33] K. Peeters, J. Sonnenschein and M. Zamaklar, “Holographic melting and related properties of mesons in a quark gluon plasma,” arXiv:hep-th/0606195.
- [34] H. Liu, K. Rajagopal and U. A. Wiedemann, “An AdS/CFT Calculation of Screening in a Hot Wind,” arXiv:hep-ph/0607062.
- [35] I. R. Klebanov, J. M. Maldacena and C. B. Thorn, “Dynamics of flux tubes in large N gauge theories,” *JHEP* **0604** (2006) 024 [arXiv:hep-th/0602255].
- [36] E. Witten, “Baryons and branes in anti de Sitter space,” *JHEP* **9807**, 006 (1998) [arXiv:hep-th/9805112].
- [37] Y. Imamura, “Supersymmetries and BPS configurations on Anti-de Sitter space,” *Nucl. Phys. B* **537** (1999) 184 [arXiv:hep-th/9807179].
- [38] C. G. Callan, A. Güijosa and K. G. Savvidy, “Baryons and string creation from the fivebrane worldvolume action,” *Nucl. Phys. B* **547** (1999) 127 [arXiv:hep-th/9810092];
C. G. Callan, A. Güijosa, K. G. Savvidy and O. Tafjord, “Baryons and flux tubes in confining gauge theories from brane actions,” *Nucl. Phys. B* **555**, 183 (1999) [arXiv:hep-th/9902197].
- [39] K. Rajagopal, private communication.
- [40] U. A. Wiedemann, private communication.

- [41] L. Susskind and E. Witten, “The Holographic Bound In Anti-De Sitter Space,” arXiv:hep-th/9805114;
A. W. Peet and J. Polchinski, “UV/IR relations in AdS dynamics,” Phys. Rev. D **59** (1999) 065011 [arXiv:hep-th/9809022].
- [42] E. Cáceres, M. Natsuume and T. Okamura, “Screening Length in Plasma Winds,” arXiv:hep-th/0607233.